Available online at www.sciencedirect.com
SCIENCE DIRECT®
Journal of Solid State Chemistry 177 (2004) 786–792
JOURNAL OF SOLID STATE CHEMISTRY
http://elsevier.com/locate/jssc

Inorganic–organic hybrids of the *p*,*p*′-diphenylmethylenediphosphinate ligand with bivalent metals: a new 2D-layered phenylphosphinate zinc(II) complex

Franco Cecconi,[a] Dainis Dakternieks,[b] Andrew Duthie,[b] Carlo A. Ghilardi,[a] Pedro Gili,[c] Pablo A. Lorenzo-Luis,[c] Stefano Midollini,[a] and Annabella Orlandini[a,*]

[a] *Istituto di Chimica dei Composti Organometallici, CNR, Polo Scientifico, Via Madonna del Piano, 50019 Sesto Fiorentino, Firenze, Italy*
[b] *Centre for Chiral and Molecular Technologies, Deakin University, Geelong, Victoria 3217, Australia*
[c] *Departamento de Quimica Inorganica, Facultad de Farmacia, Universidad de La Laguna, 38204-La Laguna, Tenerife, Canary Islands, Spain*

Received 17 July 2003; accepted 17 September 2003

Abstract

By reaction of $Zn(CH_3COO)_2$ with *p*,*p*′-diphenylmethylenediphosphinic acid in water a new inorganic–organic polymeric hybrid of formula $[Zn(CH_2(P(Ph)O_2)_2)]$ has been synthesized and completely characterized. The X-ray analysis established that the structure consists of 2D-layered polymeric array, the 2D-sheets being built up through strong covalent linkages between the zinc metal and the oxygen donors of the phenylphosphinate ligand. The 2D-layers, which are featuring a mesh-net fashion, present voids of various dimensionality, up to 24-membered rings. The organic parts of the hybrid ligand, namely the phenyl rings, are shielding the inorganic skeleton of the layers, preventing the propagation of the polymer in the third dimension. No water molecules are present in the lattice, both of coordination and crystallization. Crystal data are: monoclinic, $P2_1/c$, $a = 11.840(2)$, $b = 9.646(9)$, $c = 12.516(5)$ Å, $\beta = 95.03(2)$, $V = 1423.9(15)$ Å^3, $Z = 4$. The solid material has been characterized by ^{31}P MAS NMR spectroscopy and thermogravimetric analysis.

Keywords: Zinc; Phosphinate; Hybrid material; X-ray structure; Thermal analysis; MAS NMR

1. Introduction

Among the inorganic–organic hybrid complexes the metal phosphonates [1–8] and/or phosphinates [9–16] represent a research field of great interest for their potential capability to be used in diverse applications (molecular sieves, selective catalysts, absorbers, ionic exchangers, matrices for electric and magnetic devices).

In particular some metal monophosphinates, owing to their aptitude to polymerization, were already known in the past to be used in the coating and grease thickeners industry [9].

However, while the metal phosphonates are characterized by a poly shaped structural typology as they are suitable to form up to 3D arrays, the phosphinates generally present polymeric monodimensional structures constructed by single, double, triple or double-ribbon bridges.

Recently, we have reported an isomorphous series of metal phosphinates complexes of formula $[M(pcp)(H_2O)_3]\cdot H_2O$, where $M = Mn(II)$, Co(II), Ni(II) and pcp is the bifunctional *p*,*p*′-diphenylmethylenediphosphinate ligand, where the structure is arranged in the form of 2D-layers [17]. Interestingly in such series the metals can be replaced by other metals without changes of the primary structure. As a matter of fact isomorphous mixed metal/pcp complexes have been also obtained. The importance of the presence in the lattice of water molecules, both of crystallization and coordination, is well recognized, as the propagation of the structures in 2D extended networks is just attributable to strong hydrogen bonding interactions. The cementing power of the H-bonding is exemplified also in another pcp complex, reported recently by us, containing the beryllium metal [18]. The removal of the water

*Corresponding author. Fax: +39-055-5225203.
E-mail address: annabella.bianchi@iccom.cnr.it (A. Orlandini).

0022-4596/$ - see front matter © 2003 Elsevier Inc. All rights reserved.
doi:10.1016/j.jssc.2003.09.011

molecules in such compounds appears of importance in the design of open coordination site moieties, which is useful in the catalytic and intercalation chemistry [19].

With the bifunctional ligand pcp we have now succeeded in synthesizing two other hybrid polymers of formula [M(pcp)], where $M = Zn(II)$ and Pb(II), characterized by the complete absence of water molecules, both of crystallization or coordination. While the Pb derivative presents a polymeric columnar 1D structure, whose description has been already published [20], the Zn complex shows a bidimensional polymeric array, characterized by 2D layers built by strong covalent linkages.

The complex has been characterized by X-ray structure determination, ^{31}P MAS NMR spectroscopy and thermogravimetric analysis.

2. Experimental

2.1. Materials

All reagents were analytical grade commercial products and were used without further purification. The p,p'-diphenylmethylenediphosphinic acid was prepared as previously described [21]. The crude material was recrystallized from 0.2 M solution of HCl to give microcrystals of $H_2pcp \cdot H_2O$.

2.2. General physical methods

Elemental analysis (C, H, N) were performed with an EA 1108 CHNS-0 automatic analyser. FT-IR spectra were recorded on a ThermoNicolet spectrometer (mod. Avatar 360 FT/IR) and the samples were prepared as KBr discs. Thermal analyses were carried out on a PerkinElmer system (mod. Pyris Diamond TG/DTA) under a nitrogen atmosphere (flow rate: 80 $cm^3 min^{-1}$) from 25°C to 550°C. The samples (ca. 4 mg) were heated in an aluminum crucible (45 μL) at a rate of 10°C min^{-1}. The TG curves were analyzed as percentage mass loss as a function of temperature. The number of decomposition steps were identified using the derivative thermogravimetric curve (DTG). The DTA curves were analyzed as differential thermal analysis ($\Delta T(\mu V)$). The ^{31}P and ^{207}Pb MAS NMR spectra were measured using a JEOL Eclipse Plus 400 spectrometer at 161.83 and 83.42 MHz, respectively, and are referenced against aqueous H_3PO_4 (90%) and $PbMe_4$ using crystalline $NH_4H_2PO_4$ (δ 0.95) and Pb(p-Tol)$_4$ (δ −148.8) as secondary references. At least two experiments with sufficiently different spinning rates, ranging from 4 to 10 kHz, were recorded in order to determine the isotropic chemical shift.

2.3. Synthesis of [Zn(pcp)]

A solution of $Zn(CH_3COO)_2 \cdot 2H_2O$ (60 mg, 0.37 mmol) in water (40 cm^3) at 363 K was added to a solution of $H_2pcp \cdot H_2O$ (116 mg, 0.37 mmol) in 40 cm^3 of the same solvent at the same temperature. Standing of the resulting solution at 363 K overnight afforded colorless crystals of Zn(pcp). These were filtered, washed with boiling water and dried in air. Yield ca. 83%. Anal. Calcd. for $C_{13}H_{12}O_4P_2Zn$: C, 43.42; H, 3.36%. Found: C, 43.46; H, 3.42%.

2.4. X-ray structure determination

Diffraction data for the zinc derivative were collected at room temperature on an Enraf Nonius CAD4 automatic diffractometer. Unit cell parameters were determined by least-squares refinement of the setting angles of 25 carefully centered reflections. Crystal data and data collection details are given in Table 1. The intensities I were assigned the standard deviations $\sigma(I)$ calculated by using a value of 0.03 for the instability factor k [22]. They were corrected for Lorentz-polarization effects and an empirical absorption correction (ψ scans) was applied [23]. Atomic scattering factors for neutral atoms were taken from Ref. [24]. Both $\Delta f'$ and $\Delta f''$ components of anomalous dispersion were included for all non-hydrogen atoms [25]. The structure was solved by direct methods and refined by full-matrix F^2 refinement, with anisotropic thermal parameters

Table 1
Crystal data and structure refinement

Empirical formula	$C_{13}H_{12}O_4P_2Zn$
Formula weight	359.54
Temperature (K)	295(2)
Wavelength	0.71073 Å
Crystal system, space group	Monoclinic, $P2_1/c$
Unit-cell dimensions	
a (Å)	11.840(2)
b (Å)	9.646(9)
c (Å)	12.516(5)
α (deg)	90
β (deg)	95.03(2)
γ (deg)	90
Volume (Å^3)	1423.9(15)
Z, Calculated density (g cm^{-3})	4, 1.677
Absorption coefficient (mm^{-1})	1.957
$F(000)$	728
Crystal size (mm)	0.40 × 0.38 × 0.10
θ range for data collection (deg)	2.67–21.98
Limiting indices	$-12 \leqslant h \leqslant 12$, $0 \leqslant k \leqslant 10$, $0 \leqslant l \leqslant 13$
Reflections collected/unique	1834/1735 [$R_{int} = 0.0352$]
Refinement method	Full-matrix least-squares on F^2
Data/restraints/parameters	1735/0/181
Goodness-of-fit on F^2	1.029
Final R indices [$I > 2\sigma(I)$]	$R_1 = 0.0329$, w$R_2 = 0.0829$
R indices (all data)	$R_1 = 0.0446$, w$R_2 = 0.0880$
Largest diff. peak and hole (e A^{-3})	0.415 and −0.475

Table 2
Atomic coordinates ($\times 10^4$) and equivalent isotropic displacement parameters ($Å^2 \times 10^3$)

	x	y	z	U_{eq}
Zn(1)	10744(1)	4864(1)	3444(1)	29(1)
P(1)	8304(1)	4766(1)	4280(1)	29(1)
P(2)	8951(1)	7011(1)	2657(1)	31(1)
O(1)	9390(2)	4082(3)	4031(2)	33(1)
O(2)	8066(2)	4754(3)	5446(2)	35(1)
O(3)	10164(2)	6547(3)	2762(2)	35(1)
O(4)	8751(2)	8549(3)	2543(2)	38(1)
C(1)	8320(4)	6556(4)	3864(3)	32(1)
C(11)	7130(3)	3979(4)	3517(3)	33(1)
C(12)	7301(4)	3067(4)	2696(3)	43(1)
C(13)	6385(4)	2544(6)	2064(4)	60(1)
C(14)	5307(5)	2945(6)	2239(5)	70(2)
C(15)	5124(4)	3858(6)	3041(5)	66(2)
C(16)	6030(4)	4376(5)	3682(4)	48(1)
C(21)	8227(3)	6148(4)	1534(3)	35(1)
C(22)	7102(4)	6457(5)	1231(4)	51(1)
C(23)	6529(5)	5802(7)	363(4)	68(2)
C(24)	7085(6)	4837(6)	−217(4)	70(2)
C(25)	8173(5)	4536(6)	70(4)	65(2)
C(26)	8758(4)	5165(5)	945(4)	48(1)

U_{eq} is defined as one-third of the trace of the orthogonalized U_{ij} tensor.

assigned to all non-hydrogen atoms. The hydrogen atoms were introduced in their calculated positions riding on their carbon atoms, with thermal parameters 20% larger than those of the respective carbon atoms. The function minimized during the refinement was $\sum w(F_o^2 - F_c^2)^2$, with $w = 1/[\sigma^2(F_o^2) + (0.0593P)^2 + 0.59P](P = (\max(F_o^2, 0) + 2F_c^2)/3)$. All the calculations were performed on a Pentium processor, using the package WINGX [26] (SIR97 [27], SHELX97 [28], ORTEP-III [29]). Table 2 reports final refined atomic parameters. Crystallographic data have been deposited with the Cambridge Crystallographic Data Centre as supplementary publication No. CCDC 220333.

3. Results and discussion

The complex, which is synthesized in water solution, is insoluble both in water and in organic solvents.

In the polymeric hybrids [M(pcp)] with $M = Zn(II)$ and Pb(II), unlike the hybrids of the isomorphous hydrated $[M(pcp)(H_2O)_3]\cdot H_2O$ ($M = Ni$, Co, Mn) series [17], there are no water molecules in the sphere of coordination nor interspersed in the lattice. The Zn and Pb structures differ dramatically, with the different spheres of coordination of the two metals playing an important role in conditioning the building of the polymeric arrangement. In the Pb derivative, whose structure has been already described in a previous communication [20] (see Fig. 1), the metal is surrounded by five oxygen atoms from four pcp ligands in a square

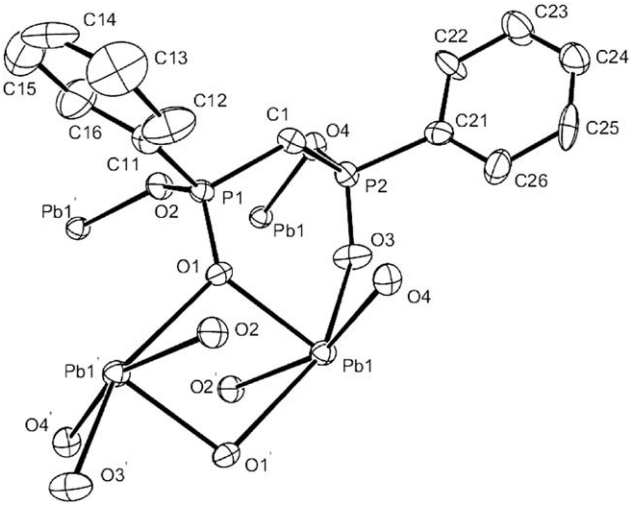

Fig. 1. Perspective view of a portion of the polymer [Pb(pcp)], showing the coordination environment of the lead atom. ORTEP-III drawing with 30% probability ellipsoids.

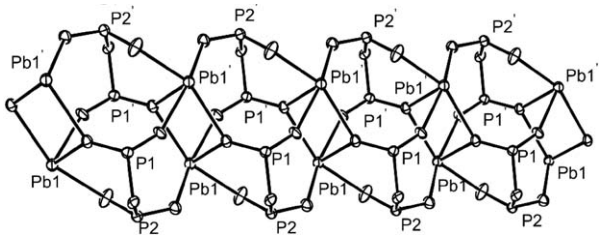

Fig. 2. Perspective view of some symmetry related units of [Pb(pcp)] showing the propagation of the 1D polymer along the b-axis.

pyramidal geometry, with an evident localization of the Pb(II) lone pair in the void left free by such hemileptic coordination. Conversely in the Zn(II) complex, the metal is surrounded by four oxygen atoms from three pcp ligand, in an homoleptic tetrahedral coordination. Starting from these units the building up of the extended networks differently proceeds in the two hybrids. While the structure of the lead(II) complex is constituted by a polymeric 1D columnar array (see Fig. 2), the column being formed by two intersecting sinusoidal ribbons of Pb atoms, bridged by the phosphinate ligand, the molecular structure of the Zn hybrid consists of 2D-layered [Zn(pcp)] polymers.

Fig. 3 shows the asymmetric unit of the zinc polymer, doubled through the center of symmetry to illustrate the complete connectivity to the metal. Selected bond distances and angles of the compound are reported in Table 3.

Each zinc metal is tetrahedrally coordinated by four phosphinate oxygen donors from three pcp ligands (one of them in a bidentate and the others in a monodentate fashion), the pcp ligand using all of its oxygen atoms. Each ZnO_4 tetrahedron is linked to other ZnO_4 moieties through bridging phosphinate groups, so that a complex

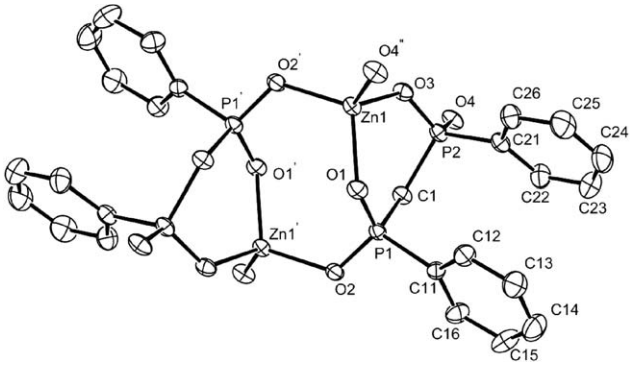

Fig. 3. Perspective view of a portion of the polymer [Zn(pcp)], showing the labeling of the asymmetric unit. ORTEP-III drawing with 30% probability ellipsoids.

Table 3
Selected bond lengths (Å) and angles(deg)

Zn(1)–O(4)#1	1.903(3)	P(1)–C(11)	1.785(4)
Zn(1)–O(2)#2	1.926(3)	P(1)–C(1)	1.805(4)
Zn(1)–O(3)	1.932(3)	P(2)–O(3)	1.499(3)
Zn(1)–O(1)	1.971(3)	P(2)–O(4)	1.507(3)
P(1)–O(1)	1.502(3)	P(2)–C(21)	1.787(4)
P(1)–O(2)	1.510(3)	P(2)–C(1)	1.798(4)
O(4)#1–Zn(1)–O(2)#2	110.12(13)	O(3)–P(2)–O(4)	116.34(17)
O(4)#1–Zn(1)–O(3)	113.18(12)	O(3)–P(2)–C(21)	108.65(18)
O(2)#2–Zn(1)–O(3)	111.54(12)	O(4)–P(2)–C(21)	108.93(19)
O(4)#1–Zn(1)–O(1)	107.40(12)	O(3)–P(2)–C(1)	108.58(18)
O(2)#2–Zn(1)–O(1)	111.78(11)	O(4)–P(2)–C(1)	104.25(17)
O(3)–Zn(1)–O(1)	102.57(12)	C(21)–P(2)–C(1)	109.93(19)
O(1)–P(1)–O(2)	115.59(16)	P(1)–O(1)–Zn(1)	130.38(17)
O(1)–P(1)–C(11)	110.08(18)	P(1)–O(2)–Zn(1)#2	120.64(17)
O(2)–P(1)–C(11)	108.16(18)	P(2)–O(3)–Zn(1)	126.20(16)
O(1)–P(1)–C(1)	109.26(17)	P(2)–O(4)–Zn(1)#3	131.42(17)
O(2)–P(1)–C(1)	107.05(17)	P(2)–C(1)–P(1)	119.5(2)
C(11)–P(1)–C(1)	106.28(19)		

Symmetry transformations used to generate equivalent atoms: #1 $-x+2$, $y-1/2$, $-z+1/2$; #2 $-x+2$, $-y+1$, $-z+1$; #3 $-x+2$, $y+1/2$, $-z+1/2$.

2D layered network results. The sheet, which is characterized by a mesh-net array, shows various voids of various dimensions. Besides the six-membered rings formed upon the chelation of the pcp ligand to the Zn center (O–P–C–P–O–Zn), there are voids created by eight- and 24-membered rings. The eight-membered rings, with a pseudo-chair conformation, are created by two zinc atoms and two phosphinate groups in an alternating array. The connectivity of the six- and eight-membered rings is depicted in Fig. 3.

From the linkage of four of the subunits represented in Fig. 3, a 24-membered moiety is created, whose connectivity is shown in Fig. 4. The phosphinate oxygens connect the zinc atoms so that six zinc atoms are alternated with six phosphinate groups O–P–O. The propagation of this portion of the polymer in the *yz* plane gives a bidimensional sheet, featuring a mesh-net. Fig. 5 shows the packing diagram of [Zn(pcp)] as viewed down the *x* axis, with exclusion of the phenyl rings for

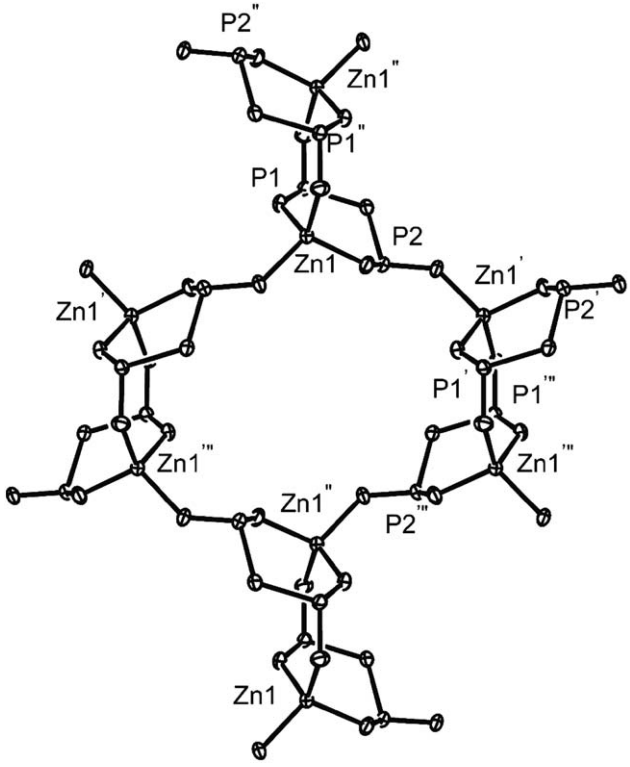

Fig. 4. Perspective view of a portion of the [Zn(pcp)] polymer showing the 24-membered ring. View normal to [100]. The phenyl rings are omitted for sake of clarity. The unlabeled atoms linked to zinc represent oxygens.

sake of clarity. Although the voids could appear large enough to be useful in intercalation chemistry, the phenyl rings project toward the pores and therefore, as it is evident from the packing diagram in which phenyls are included (Fig. 6), reduce the size of the voids. A schematic packing of the polymer with view down the *y* axis is represented in Fig. 7. It is evident that interruption of the structure in the third dimension is caused by shielding from hydrophobic region of the ligand (phenyl rings) on the inorganic part of the hybrid polymer.

In regard to the coordination of the zinc(II) metal, a little distortion from the limit tetrahedral geometry is represented by the spread of the O–Zn–O angles between 102.57(12)° and 113.18(12)°. The Zn–O bond distances from 1.903(3) to 1.971(3) Å appear comparable with analogous linkages, in other Zn/phosphonates reported [30]. Concerning the pcp ligand, bond distances and angles exhibit expected values; in particular the P–O bonds appear all very similar, in agreement with the nature of the linkages displayed.

In summary, while several structures of zinc/phosphonates hybrid complexes are known, very few zinc/phosphinates have been reported [16,31–34] and are generally characterized by monodimensional polymeric chains with single, double or triple phosphinate bridges.

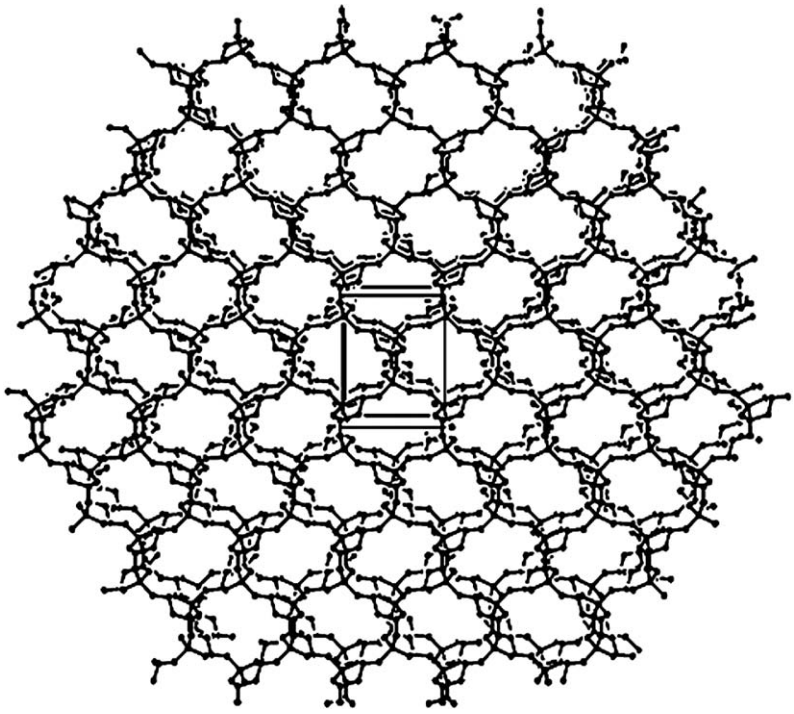

Fig. 5. Perspective view of a portion of the [Zn(pcp)] polymer showing the propagation of the layer in the *yz* plane. Phenyl rings are omitted for sake of clarity.

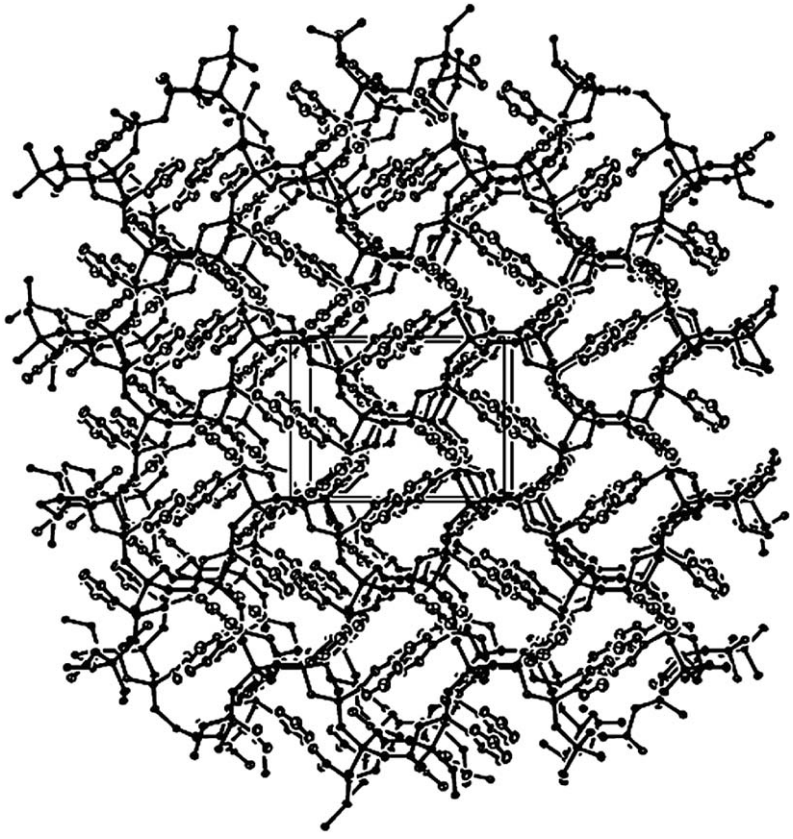

Fig. 6. Packing diagram of [Zn(pcp)] with view normal to [100].

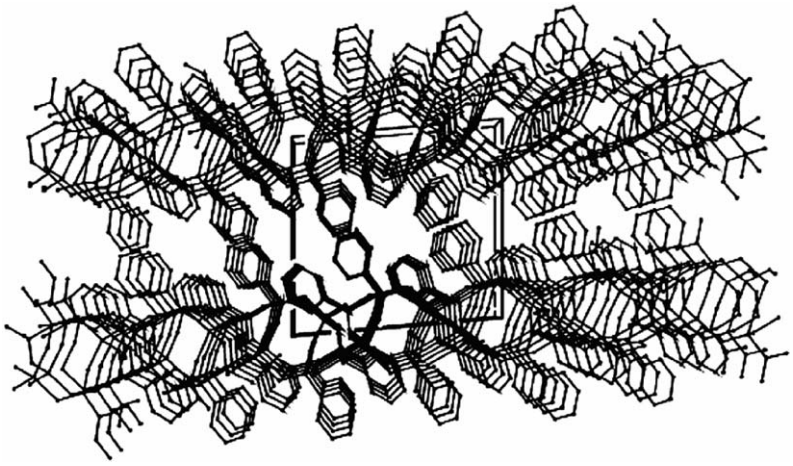

Fig. 7. Packing diagram of [Zn(pcp)] with view normal to [010].

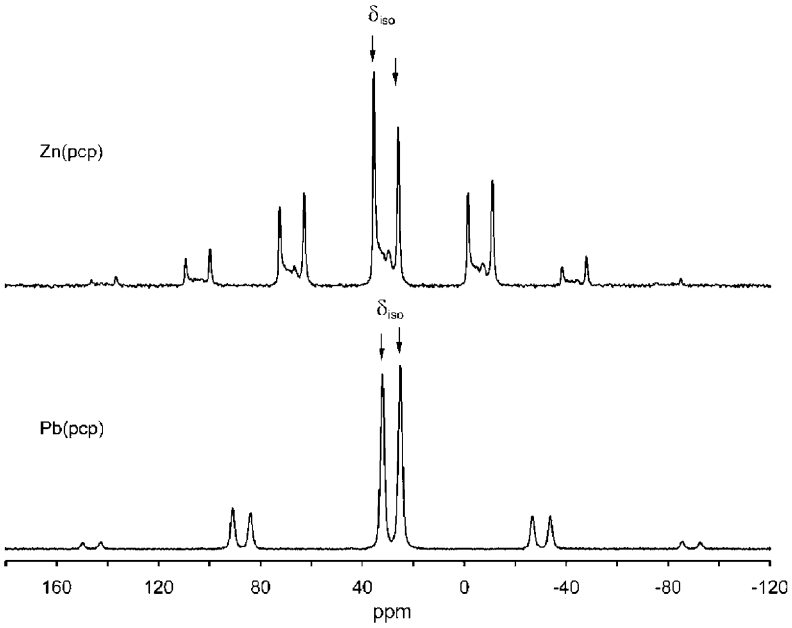

Fig. 8. ^{31}P MAS NMR spectra (161.83 MHz) of [Zn(pcp)] and [Pb(pcp)] at spinning speeds of 6.0 and 9.6 kHz, respectively.

MAS NMR spectra and TG-DTG/DTA analyses of the [Zn(pcp)] complex and of the related [Pb(pcp)] derivative were performed for comparison purposes.

The ^{31}P MAS NMR spectra of both compounds are shown in Fig. 8. The presence of two phosphorus signals at 24.5 and 31.4 ppm in the spectrum of Pb complex indicates that the two phosphorus atoms of the ligand are inequivalent, as actually found in the X-ray results. Analogously in the spectrum of the Zn derivative there are two main signals (80–90%) at 25.9 and 35.5 ppm, attributable to the inequivalent phosphorus atoms. However, other minor resonances overlapping the principal ones show the presence at least of another polymorphic form of [Zn(pcp)]. The formation of polymorphic phases has been previously observed in Zn/phosphonate polymers [33]. As we have found a resonance at 32.8 ppm in the ^{31}P MAS NMR of solid H_2pcp (vs. 28.0 ppm in DMSO solution), there is not much variation in the position of the ^{31}P MAS NMR signal for H_2pcp, [Zn(pcp] and [Pb(pcp)] compounds. The difference between the chemical shifts of H_2pcp in solution and in the solid state may be ascribed to the presence of hydrogen bonds in the solid state.

The ^{207}Pb MAS NMR spectrum of [Pb(pcp)] shows an extremal broad signal at -2675 ppm ($W_{1/2} =$ 5000 Hz). The value of the chemical shift appears to be consistent with the values reported for other lead containing compounds, as the donor oxygen atoms of pcp are remarkable electronegative [35,36].

The [Zn(pcp)] and [Pb(pcp)] compounds show a very similar thermogravimetric behavior. The TG-DTG/DTA curves for both compounds reveal no presence

Table 4
Thermal data of decomposition processes for [Zn(pcp)] **1** and [Pb(pcp)] **2**

First and second steps Complex	Temp. range (°C)	Temp. of the DTG peak (°C)	Loss of wt% found	Temp. of endothermic peak (°C)	Temp. of exothermic peak (°C)
1	25–434	—	—	—	—
2	25–411	—	—	—	—
				Temp. of exothermic peak (°C)	
1	434–550	488	29.41%	476 and 494	
2	411–550	439	33.0%	449, 488 and 507	

of endothermic or exothermic peaks up to 411–434°C, indicating the absence of water molecules, both of crystallization and coordination (see Figs. 9 and 10 in Supplementary Material). At higher temperatures pyrolisis of the organic part of the complexes takes place, with changing of the color to black. Thermal data of the decomposition processes for both compounds are reported in Table 4. A comparison of the IR spectra before and after the combustion, evidences the presence of a new band at 1650 cm^{-1}, whereas other bands disappear in the regions 3050–3060 [aromatic ν(C–H)], 1150 [ν(P–C)], 1430–1440 [phenyl ν(C=C)] cm^{-1}, probably due to oxidation of the remaining organic matter [37,38]. The band at 1650 cm^{-1} may be due to an overtone or combination band of the CPO_3 stretching vibrations or due to the bending vibration of the PO–H–OP group, which interacts strongly by H-bonding [39]. The analysis of this material shows the presence of carbon (ca. 12%) and hydrogen (ca. 1.8%), probably due to an incomplete combustion in our conditions.

References

[1] A. Clearfield, in: K.D. Karlin (Ed.), Progress in Inorganic Chemistry, Vol. 47, Wiley, New York, 1998, p. 371.
[2] A. Cabeza, M.A.G. Aranda, S. Bruque, J. Mater. Chem. 8 (1998) 2479.
[3] C.V.K. Sharma, A. Clearfield, A. Cabeza, M.A.G. Aranda, S. Bruque, J. Am. Chem. Soc. 125 (2001) 2885.
[4] A. Cabeza, X. Ouyang, C.V.K. Sharma, M.A.G. Aranda, S. Bruque, A. Clearfield, Inorg. Chem. 41 (2002) 2325.
[5] S. Ayyappan, G. Diaz de Delgado, A.K. Cheetman, G. Ferey, C.N.R. Rao, J. Chem. Soc. Dalton Trans. (1999) 2905.
[6] R. LaDuca, D. Rose, J.R.D. Debord, R.H. Haushalter, C.J. O'Connor, C.J. Zubieta, J. Solid State Chem. 123 (1996) 408.
[7] J.-G. Mao, Z. Wang, A. Clearfield, Inorg. Chem. 41 (2002) 6106.
[8] J.-G. Mao, A. Clearfield, Inorg. Chem. 4 (2002) 2319 (and references therein).
[9] B.P. Block, Inorg. Macromol. Rev. 1 (1970) 115.
[10] P. Colamarino, P.L. Orioli, W.D. Benzinger, H.D. Gillman, Inorg. Chem. 15 (1976) 800.
[11] R. Cini, P. Colamarino, P.L. Orioli, L.S. Smith, P.R. Newman, H.D. Gillman, P. Nannelli, Inorg. Chem. 16 (1977) 3223.
[12] S.-J. Lin, R.J. Staples, J.P. Fackler Jr., Polyhedron 11 (1992) 2427.
[13] V. Chandrasekhar, A. Chandrasekaran, R.O. Day, J.M. Holmes, R.R. Holmes, Phosphorus Sulfur Silicon Relat. Elem. 115 (1996) 125.
[14] K.W. Oliver, S.J. Rettig, R.C. Thomson, J. Trotter, S. Xuia, Inorg. Chem. 36 (1997) 2465.
[15] D. Grohol, F. Gingl, A. Clearfield, Inorg. Chem. 38 (1999) 751.
[16] M. Shieh, K.J. Martin, P.J. Squattrito, A. Clearfield, Inorg. Chem. 29 (1990) 958.
[17] E. Berti, F. Cecconi, C.A. Ghilardi, S. Midollini, A. Orlandini, E. Pitzalis, Inorg. Chem. Commun. 3 (2002) 1041.
[18] F. Cecconi, S. Dominguez, N. Masciocchi, S. Midollini, A. Sironi, A. Vacca, Inorg. Chem. 42 (2003) 2350.
[19] G. Cao, T.E. Mallouk, Inorg. Chem. 30 (1991) 1434.
[20] F. Cecconi, C.A. Ghilardi, S. Midollini, A. Orlandini, Inorg. Chem. Commun. 6 (2003) 546.
[21] M.E. Garst, Synth. Commun. 9 (1979) 261.
[22] P.W.R. Corfield, R.J. Doedens, J.A. Ibers, Inorg. Chem. 6 (1967) 197.
[23] A.C.T. North, D.C. Phillips, F.S. Mathews, Acta Crystallogr. A 24 (1968) 351.
[24] A.J.C. Wilson, International Tables for X-ray Crystallography, Vol. C, Kluwer Academic Publishers, Dordrecht, 1992, p. 500.
[25] A.J.C. Wilson, International Tables for X-ray Crystallography, Vol. C, Kluwer Academic Publishers, Dordrecht, 1992, p. 219.
[26] L.J. Farrugia, J. Appl. Crystallogr. 32 (1999) 876.
[27] A. Altomare, M.C. Burla, M. Camalli, G.L. Cascarano, C. Giacovazzo, A. Guagliardi, A.G.C. Moliterni, G. Polidori, G.R. Spagna, J. Appl. Crystallogr. 32 (1999) 115.
[28] G.M. Sheldrick, SHELX97, University of Göttingen, Göttingen, Germany, 1997.
[29] M.N. Burnett, C.K. Johnson, ORTEP-III, Oak Ridge National Laboratory, Oak Ridge, TN, 1996.
[30] D.M. Poojary, B. Zhang, A. Clearfield, Chem. Mater. 11 (1999) 421.
[31] V. Giancotti, F. Giordano, L. Randaccio, A. Ripamonti, J. Chem. Soc. A (1968) 757.
[32] F. Giordano, L. Randaccio, A. Ripamonti, Acta Crystallogr. Sect. B 25 (1969) 1057.
[33] R. Cini, P.L. Orioli, M. Sabat, H.D. Gillman, Inorg. Chim. Acta 59 (1982) 225.
[34] E. Cole, R.C.B. Copley, J.A.K. Howard, D. Parker, G. Ferguson, J.F. Gallagher, B. Kaitner, A. Harrison, L. Royle, J. Chem. Soc. Dalton Trans. (1994) 1619.
[35] F. Fayon, I. Farnan, C. Bessada, J. Coutures, D. Massiot, J.P. Coutures, J. Am. Chem. Soc 119 (1997) 6837.
[36] G.D. Fallon, L. Spiccia, B.O. West, Q. Zhang, Polyhedron 16 (1997) 19.
[37] F. Cecconi, C.A. Ghilardi, P. Gili, S. Midollini, P.A. Lorenzo-Luis, A.D. Lozano-Gorrìn, A. Orlandini, Inorg. Chim. Acta 319 (2001) 67.
[38] G.B. Hix, S.J. Kitchin, K.D.M. Harris, J. Chem. Soc. Dalton Trans. (1998) 2315.
[39] A. Cabeza, M.A.G. Aranda, S. Bruque, J. Mater. Chem. 9 (1999) 571.